ANALYSIS OF THE MULTIPHASE INDUCTOR-CONVERTER BRIDGE

by

Mehrdad Ehsani, Robert L. Kustom, and Raymond E. Fuma

Prepared for

Second International Pulsed Power Conference

Lubbock, Texas

12-14 June 1979

MASTER

ARGONNE NATIONAL LABORATORY, ARGONNE, ILLINOIS

U of C-AUA-USDOE

Operated under Contract W-31-109-Eng-38 for the

U. S. DEPARTMENT OF ENERGY

DISCLAIMER

This report was prepared as an account of work sponsored by an agency of the United States Government. Neither the United States Government nor any agency Thereof, nor any of their employees, makes any warranty, express or implied, or assumes any legal liability or responsibility for the accuracy, completeness, or usefulness of any information, apparatus, product, or process disclosed, or represents that its use would not infringe privately owned rights. Reference herein to any specific commercial product, process, or service by trade name, trademark, manufacturer, or otherwise does not necessarily constitute or imply its endorsement, recommendation, or favoring by the United States Government or any agency thereof. The views and opinions of authors expressed herein do not necessarily state or reflect those of the United States Government or any agency thereof.

DISCLAIMER

Portions of this document may be illegible in electronic image products. Images are produced from the best available original document.

ANALYSIS OF THE MULTIPHASE INDUCTOR-CONVERTER BRIDGE*

Mehrdad Ehsani,[†] Robert L. Kustom, and Raymond E. Fuja

Argonne National Laboratory
Argonne, Illinois 60439

Abstract

Analytical derivations are presented for inductor-converter bridge (ICB) circuits in which energy is transferred from a storage inductor to a load inductor with solid state bridges. These derivations provide complete analytical circuit solution in contrast to previously available numerical (non-analytical) procedures. The analysis is based on two parallel methods: (1) Fourier expansion of the inverter waveforms and (2) a novel method based on the inherent waveforms of the ICB, labeled square functions. Our analytical values of power flow, inductor currents, and voltages compare favorably with the results of a three-phase ICB experiment at Argonne National Laboratory.

Introduction

The inductor-converter bridge (ICB) is a solid state dc-ac-dc converter system for reversible energy transfer between two inductors. This system is especially suitable for pulsed power supply applications greater than several hundred megawatts and durations from a fraction of a second to many seconds. Two such applications are the superconductive equilibrium field coils of the projected tokamak fusion power reactors and superconductive magnets to be used in future particle accelerators.

The ICB system is inherently efficient, controllable in real time and allows isolation of large

---

pulsed reactive loads from the power grid. Thus, only the average system losses are drawn from the grid.

Operation of the ICB Circuit

Detailed operation of the ICB may be found in references 1 and 2. Figure 1 shows a three-phase ICB where the storage and the load coil is represented by L_S and L_L, respectively. At a typical instant during the energy transfer, dc currents i_S and i_L will be flowing in the storage and load coils, respectively. The SCR's of the left hand side (storage side) are fired in the normal Graetz bridge sequence: S_{L1} S_{L5}, S_{L1} S_{L6}, S_{L2} S_{L6}, S_{L2} S_{L4}, S_{L3} S_{L4}, S_{L3} S_{L5}, S_{L1} S_{L5}, ····
The SCR's of the right-hand side (load side) follow the same sequence but may be out of step with respect to the storage side. The direction and the level of power flow is determined by the relative timing between the source and the load bridge switching sequences such that a load bridge lead will cause power flow into the load and vice versa. The Y-connected capacitors in the middle serve as the intermediate energy store between the storage and load coils and they provide the reverse voltages to commutate the inductor circuits from one SCR to the next. Thus, no external counterpulse circuit is needed.

Only a very small fraction of each coil energy is extracted in each bridge cycle. Therefore, by varying the relative timing between the source and load switching sequences and/or the frequency of operation, very fine control over the rate of energy transfer can be achieved. The functional dependence of the power on the relative timing

1

(relative phase difference) and the frequency will be illustrated in the following sections.

Circuit Analysis Based on Fourier Components

Figure 2 shows an m-phase ICB. For this analysis, the SCR's have been replaced by ideal switches. This idealization implies a lossless system and operation within the successful commutation bounds. Since each bridge cycle changes the coil energies by a very small amount, the inductor currents are nearly constant in one cycle. Viewing such inductor-converter half from the m-phase ac lines, one will see an m-phase square wave current source system, each phase being $\frac{2\pi}{m}$ radians displaced from the next and the wave amplitude being equal to the instantaneous coil current, Fig. 3. Since the average power is divided equally between the phases, it may be calculated from a one-phase diagram, Fig. 4.

The calculated instantaneous average power from the left-hand source (storage) to the right-hand source (load) is

$$\langle p_{Sa}(t) \rangle = \sum_n \frac{1}{2n\omega c}(a_{nSa}\, b_{nLa} - b_{nSa}\, a_{nLa})$$

where the a's and b's are the Fourier coefficients of the storage and load source waveforms as indicated by the subscripts. For illustration, the Fourier coefficients of the symmetrical waveform of Fig. 5 which is for when m is odd will be used.

$$\begin{cases} I_{Sa}(t) = \sum_n \frac{2I_S}{\pi n}\left[1 - (-1)^n\right]\sin\frac{n\pi}{m}\cos n\,\omega t \\[2ex] I_{La}(t) = \sum_n \frac{2I_L}{m\pi}\left[1 - (-1)^n\right]\sin\frac{n\pi}{m}\cos n\,(\omega t + \alpha) \end{cases}$$

where α is the angle by which the load bridge leads the storage bridge. After substitution, the average power per phase will simplify to

$$\langle p_{Sa}(t) \rangle = \sum_n \frac{2I_S I_L}{n^3\pi^2\omega c}\left[1 - (-1)^n\right]^2 \left(\sin\frac{n\pi}{m}\right)^2 \sin n\alpha$$

The total instantaneous average power delivered from the storage coil is m times the above, or

$$\langle p_S(t) \rangle = \sum_n \frac{2m\, I_S I_L}{n^3\pi^2\omega c}\left[1 - (-1)^n\right]^2 \left(\sin\frac{n\pi}{m}\right)^2 \sin n\alpha.$$

The effect of the relative phase, α, and the bridge switching frequency, ω, on the power flow is evident in the above relationship. Note also that the contribution of higher harmonics is attenuated by the $\frac{1}{n^3}$ term. Figure 6 represents the plot of the instantaneous average power as a function of α with the number of phases, m, as the parameter. For m = 3, over 99.5% of the net power is delivered by the fundamental frequency, making the m = 3 curve in Fig. 6 almost purely sinusoidal.

The time functions of average coil currents, power, and voltages may now be calculated. For simplicity, let

$$k = \sum_n \frac{2m}{n^3\pi^2\omega c}\left[1 - (-1)^n\right]^2 \left(\sin\frac{n\pi}{m}\right)^2 \sin n\alpha.$$

Then from

$$\langle p_S(t) \rangle = -\frac{d\,E_{S}(t)}{dt} = \frac{d\,E_{L}(t)}{dt} \quad,$$

$$\begin{cases} k\,\langle i_S \rangle\langle i_L \rangle = -\frac{d}{dt}\left(\frac{1}{2}L_S\,\langle i_S \rangle^2\right) \\[3ex] k\,\langle i_S \rangle\langle i_L \rangle = \frac{d}{dt}\left(\frac{1}{2}L_L\,\langle i_L \rangle^2\right) \end{cases}$$

Solving these equations with the initial conditions

$$\begin{cases} \langle i_S \rangle\,\big|_{t=0} = I_o = \text{initial storage current} \\[2ex] \overset{\circ}{\langle i_S \rangle}\,\big|_{t=0} = o \quad, \end{cases}$$

we obtain

$$\begin{cases} <i_S>(t) = I_0 \cos \dfrac{K}{\sqrt{L_S L_L}} \, t \\[3mm] <i_L>(t) = I_0 \sqrt{\dfrac{L_S}{L_L}} \sin \dfrac{K}{\sqrt{L_S L_L}} \, t. \end{cases}$$

The average power will become

$$<P_S>(t) = 1/2 \, K \, I_0^2 \sqrt{\frac{L_S}{L_L}} \sin \frac{2K}{\sqrt{L_S L_L}} \, t$$

and the average coil voltages from

$$<v> = L \, \frac{d<i>}{dt} \, ,$$

$$\begin{cases} <v_S>(t) = K \, I_0 \sqrt{\dfrac{L_S}{L_L}} \sin \dfrac{k}{\sqrt{L_S L_L}} \, t \\[4mm] <v_L>(t) = K \, I_0 \cos \dfrac{k}{\sqrt{L_S L_L}} \, t \end{cases}$$

Circuit Analysis Based on Square Function Calculations

The preceding Fourier method shows the influence of harmonics in the system. However, for real time control, solving the equations of the form

$$<p> = \sum_n f_n (\alpha)$$

for α is time consuming and possibly inaccurate. The following technique will provide closed form equations that are efficiently solved by a microcomputer in real time control.

The calculations are based on specially tailored functions symbolized by Sq (X) and Tr (X), Fig. 7. These waveforms are inherent in the operation of the ICB circuits. The Sq function is a good mathematical representation of the ac phase currents of the system. The Tr function is the integral form of Sq and is a good representation of the capacitor voltages due to the phase currents. A brief mathematical development of the Sq and Tr functions is presented in the Appendix.

Figure 8 shows how a phase current of the equivalent three-phase circuit may be decomposed into two Sq functions. Thus, the currents i_{Sa} and i_{La} of Fig. 4 may be written as

$$\begin{cases} i_{Sa}(t) = \dfrac{I_S}{2} \left[\text{Sq} \left(\tau + \dfrac{T}{6} - \tau_0 \right) + \text{Sq} \left(\tau - \tau_0 \right) \right] \\[4mm] i_{La}(t) = \dfrac{I_L}{2} \left[\text{Sq} \left(\tau + \dfrac{T}{6} \right) + \text{Sq} \left(\tau \right) \right], \end{cases}$$

$$o \le t \le T, \ o \le \tau \le T, \ o \le \tau \le 1/2$$

where τ_0 is the relative lag time of the storage bridge.

These current representations for one period are adequate for instantaneous average power calculations. The net power out of storage per phase, results from the interaction of i_{Sa} and v_{La}, the capacitor voltage due to the load phase current:

$$v_{La}(t) = \frac{1}{C} \int_0^t i_{La} \, d\tau = \frac{I_L}{2C} \left[\text{Tr} \left(\tau + \frac{T}{6} \right) + \text{Tr} (t) \right].$$

This power is

$$P_{Sa}(t) = i_{Sa} v_{La} = \frac{I_S I_L}{4C} \left[\text{Sq} \left(\tau + \frac{T}{6} - \tau_0 \right) \cdot \text{Tr} \left(\tau + \frac{T}{6} \right) \right.$$
$$+ \, \text{Sq} \left(\tau + \frac{T}{6} - \tau_0 \right) \cdot \text{Tr} (\tau) + \text{Sq} \left(\tau - \tau_0 \right)$$
$$\left. \cdot \, \text{Tr} \left(\tau + \frac{T}{6} \right) + \text{Sq} \left(\tau - \tau_0 \right) \cdot \text{Tr} (\tau) \right].$$

The instantaneous average power per phase is

$$<P_{Sa}> = \frac{1}{T} \int_0^T i_{Sa} v_{La} \, dt = \frac{I_L I_S}{4TC} \int_0^T \left[\text{Sq} \left(\tau + \frac{T}{6} - \tau_0 \right) \right.$$
$$\cdot \, \text{Tr} \left(\tau + \frac{T}{6} \right) + \text{Sq} \left(\tau + \frac{T}{6} - \tau_0 \right) \cdot \text{Tr} (\tau) +$$
$$\text{Sq} \left(\tau - \tau_0 \right) \cdot \text{Tr} \left(\tau + \frac{T}{6} \right) + \text{Sq} \left(\tau - \tau_0 \right)$$
$$\left. \cdot \, \text{Tr} (\tau) \right] \, d\tau.$$

The four terms in the integrand are first transformed to the normalized variable functions shown in the Appendix, then each term is evaluated by using the proper integral identity in the Appendix. The result is then multiplied by three for the total three-phase power

$$
\langle P_{Sa} \rangle = \begin{cases} \dfrac{T\, I_S T_L}{C}\, (2\,\gamma_o - 3\,\gamma_o^2), & o \leq \gamma \leq \dfrac{1}{6} \\[2mm] \dfrac{T\, I_S I_L}{C}\, (3\,\gamma_o - 6\,\gamma_o^2 - \dfrac{1}{12}), & \dfrac{1}{6} \leq \gamma \leq \dfrac{1}{3} \\[2mm] \dfrac{T\, I_S I_L}{C}\, (\gamma_o - 3\,\gamma_o^2 + \dfrac{1}{4}), & \dfrac{1}{3} \leq \gamma \leq \dfrac{1}{2} \end{cases}
$$

where $\gamma_o = \dfrac{\tau_o}{T} = \dfrac{\alpha}{360^\circ}$ is the normalized lag time of
the storage bridge relative to the load bridge and
the frequency is represented by the period T.
This is the closed form of the <p> vs α curve for
m = 3 in Fig. 6. The time functions of the
average coil currents, power and voltages may be
calculated as before. The only difference being
that K (γ_o) is in closed form.

Expressing the actual circuit waveforms
analytically, allows other useful calculations
such as the actual capacitor voltages throughout
the transfer cycle, the study of commutation
throughout the cycle, and the actual coil voltages
and instantaneous currents, without resorting to
numerical procedures.

Comparison with Test Results

A model three-phase ICB has been built and tested
at Argonne National Laboratory. This system uses
two identical superconducting coils capable of
storing 125 kJ at 250 A, as the storage and load
inductors. Other system parameters are:

$$L_S = L_L = 4 \text{ H}, \quad I_o = 100 \text{ A}$$

$$C = 10^{-4} \text{ F}, \quad \alpha = 90^\circ$$

$$\omega = 4084 \text{ rad/s}$$

The system equations are derived from substitution
of these parameters and m = 3 into the time
functions shown in the Fourier analysis section:

$$\langle i_S \rangle (t) = 100 \cos 0.5609\, t \qquad \text{A}$$
$$\langle i_L \rangle (t) = 100 \sin 0.5609\, t \qquad \text{A}$$
$$\langle v_S \rangle (t) = 224.4 \sin 0.5609\, t \qquad \text{V}$$

$$\langle v_L \rangle (t) = 224.4 \cos 0.5609\, t \qquad \text{V}$$
$$\langle p_S \rangle (t) = 11218 \sin 1.1218\, t \qquad \text{W}$$

A plot of these equations appears in Fig. 9.

Figure 10 shows the average coil voltages and
currents obtained experimentally. Good agreement
exists between the analytical and the experimental
results. Note, however, that the experimental
initial storage current is somewhat higher than
the final load current. This is due to the losses
in the system which is neglected in this analysis,
but may be incorporated in the differential
equations leading to the average time functions.

Conclusions

The behavior of the multiphase inductor–converter
bridges have been studied by two analytical
techniques. The conventional Fourier technique
produces the average circuit power, currents, and
voltages as a function of time. It also shows the
effect of the existing harmonics in the circuit
behavior. The square function technique is
particularly devised for the ICB and other SCR
circuits in which rectangular waveforms appear.
The identities defined on the special functions
Sq (X) and Tr (X) operate directly on the circuit
waveforms. Thus, much more information about
instantaneous behavior of the circuit is available
for analysis, system design, and the development
of real time control algorithms. Preliminary
tests with open loop microcomputer control have
been conducted with satisfactory results. The
development of an optimal closed loop control
algorithm is currently in progress.

Appendix

The Sq function is defined as the sum of unit step
functions as follows,

$$\text{Sq}\ (\gamma + \gamma_o) \overset{\Delta}{=} u\ (\gamma) - 2\, u\ (\gamma - \dfrac{1}{2} + \gamma_o) + 2$$

$$u\ (\gamma - 1 + \gamma_o) - u\ (\gamma_o - 1)\ ,$$

$$0 \leq \gamma_o \leq \dfrac{1}{2}\ ,\ 0 < \gamma \leq 1.$$

The Tr function is defined as the integral value of the Sq functions,

$$Tr(\gamma + \gamma_o) \triangleq \int_0^\gamma Sq(\xi + \gamma_o) \, d\xi$$

$$= \gamma \, u(\gamma) - 2\left(\gamma - \frac{1}{2} + \gamma_o\right)$$

$$u\left(\gamma - \frac{1}{2} + \gamma_o\right) + 2(\gamma - 1 + \gamma_o)$$

$$u(\gamma - 1 + \gamma_o) - (\gamma - 1) \, u(\gamma - 1)$$

The following integral is extensively used in calculating the average power flow in the circuits of interest. Therefore, it will be stated as an identity which may be directly verified,

$$\int_0^1 [Sq(\gamma + \gamma_1) \cdot Tr(\gamma + \gamma_2)] \, d\gamma = \begin{cases} -2\gamma_1^2 - \gamma_1 + 4\gamma_1\gamma_2 + \gamma_2 \\ \quad - 2\gamma_2^2, \ \gamma_1 \leq \gamma_2 \\ \\ 2\gamma_2^2 - \gamma_1 - 4\gamma_1\gamma_2 + \gamma_2 \\ \quad + 2\gamma_2^2, \ \gamma_1 \geq \gamma_2 \ , \end{cases}$$

$$0 \leq \gamma \leq \frac{1}{2} \ , \ 0 \leq \gamma_2 \leq \frac{1}{2}.$$

The following identities will also be of considerable value

$$Sq(\gamma - \gamma_o) = - Sq[\gamma + (1/2 - \gamma_o)],$$

$$Tr(\gamma - \gamma_o) = - Tr[\gamma + (1/2 - \gamma_o)], \ 0 \leq \gamma_o \leq \frac{1}{2}$$

which may be verified by direct substitution. Note that by using these identities, we can easily evaluate the above integral for any combination of leading and lagging functions.

The above Sq and Tr functions have been defined for a period equal to 1. For periods other than 1, the argument should be multiplied by the appropriate constant:

$$Sq(t + t_o) = Sq(\gamma + \gamma_o), \begin{cases} 0 \leq t \leq T, \ 0 \leq t_o \leq \frac{T}{2} \\ \\ 0 \leq \gamma \leq 1, \ 0 \leq \gamma_o \leq \frac{1}{2} \end{cases}$$

$$Tr(t + t_o) = \int_0^t Sq(\sigma + t_o) \, d\sigma, \begin{cases} 0 \leq t \leq T \\ \\ 0 \leq t_o \leq \frac{T}{2} \end{cases},$$

where $\gamma = \dfrac{t}{T}$ and $\gamma_o = \dfrac{t_o}{T}$.

Substitution of γ and γ_o in the above integral will give

$$Tr(t + t_o) = T\int_0^\gamma Sq(\xi + \gamma_o) \, d\xi$$

$$= T[Tr(\gamma + \gamma_o)] = t \, u(t) - 2$$

$$\left(t - \frac{T}{2} + t_o\right) U\left(t - \frac{T}{2} + t_o\right)$$

$$+ 2(t - T + t_o) \, u(t - T + t_o)$$

$$- (t - T) \, u(t - T).$$

For time base calculations, these functions may be used.

References
1. R. L. Kustom et al., "The Use of Multiphase Inductor-Converter Bridges as Actively Controlled Power Supplies for Tokamak Coils," Argonne National Laboratory Report ANL/FPP/TM-78 (April 11, 1977.).
2. H. A. Peterson et al., "Superconductive Inductor-Converter Units for Pulsed Power Loads," Proceedings of International Conference on Energy Storage, Compression and Switching, Asti-Torino, Italy (November 1974).
3. M. Ehsani, R. L. Kustom, "Analysis of the Multiphase Inductor-Converter Bridge," Argonne National Laboratory Report ANL/FPP/TM-114 (August 1978).
4. M. Ehsani, R. L. Kustom, "Square Function Analysis of the Inductor-Converter Bridge," Argonne National Laboratory Report ANL/FPP/TM-118 (March 1979).
5. N. Mohan, H. A. Peterson, "Superconductive Inductor Storage and Converters for Pulsed Power Loads," Proceedings of the International Pulsed Power Conference, Lubbock, TX (November 1976).
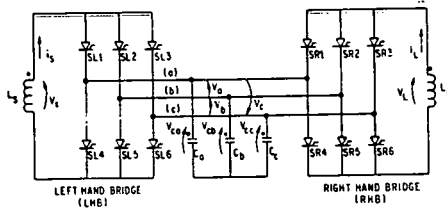
Fig. 1. Circuit Diagram for the 3-Capacitor Model IC Bridge.
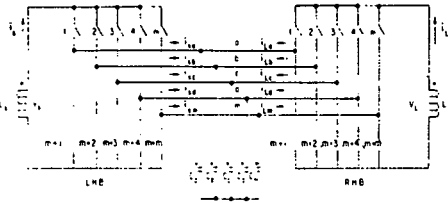

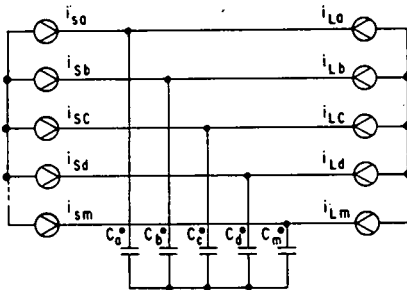Fig. 2. Circuit Diagram for an m-phase ICB.
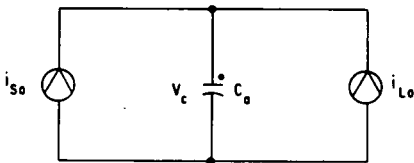

Fig. 3. Equivalent Diagram of an m-phase ICB.

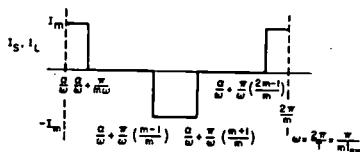

Fig. 4. One Phase Equivalent Circuit of an m-phase ICB.

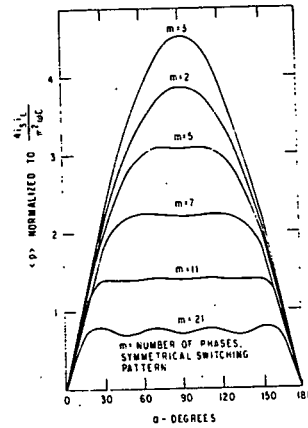Fig. 5. Single Phase Current Source Waveform for an m-phase ICB Circuit.
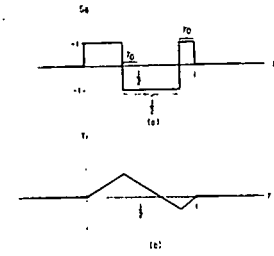

Fig. 6. Plot of <p> vs α.

Fig. 7. (a) Sq $(\gamma + \gamma_0)$,
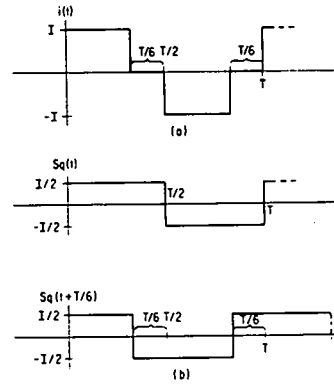
(b) Tr $(\gamma + \gamma_0)$.

Fig. 8.

(a) Phase Current in a Three-Phase ICB

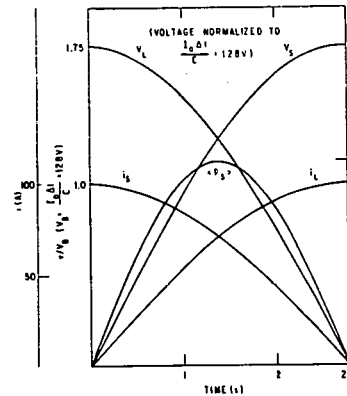(b) Decomposition of the Phase Current into Two Sq Functions.
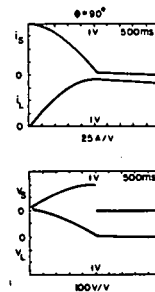

Fig. 9.

Average Coil Currents, Voltages, and Power vs Time.

Fig. 10.

Experimental Average Coil Voltage and Current Traces.

6